IEEE Access
Multidisciplinary | Rapid Review | Open Access Journal

Received July 5, 2019, accepted July 18, 2019, date of publication July 29, 2019, date of current version August 15, 2019.

Digital Object Identifier 10.1109/ACCESS.2019.2931773

A Sensitive Potentiometric Biosensor Using MBs-AO/GO/ZnO Membranes-Based Arrayed Screen-Printed Electrodes for AA Detection and Remote Monitoring

JUNG-CHUAN CHOU[1], (Senior Member, IEEE), SI-HONG LIN[1], PO-YU KUO[1], (Member, IEEE), CHIH-HSIEN LAI[1], (Member, IEEE), YU-HSUN NIEN[2], (Member, IEEE), TSU-YANG LAI[1], AND TZU-YU SU[2]

[1]Graduate School of Electronic Engineering, National Yunlin University of Science and Technology, Douliu 64002, Taiwan
[2]Graduate School of Chemical and Materials Engineering, National Yunlin University of Science and Technology, Douliu 64002, Taiwan

Corresponding author: Jung-Chuan Chou (choujc@yuntech.edu.tw)

This work was supported in part by the Ministry of Education, Taiwan, R.O.C., under Grant 107-A055-8, and in part by the Ministry of Science and Technology, Taiwan, R.O.C., under Grant MOST 107-2221-E-224-030 and Grant MOST 108-2221-E-224-020.

ABSTRACT In this paper, we used sputtering and screen-printing technology to develop a sensitive potentiometric ascorbic acid (AA) biosensor with the magnetic beads-ascorbate oxidase/graphene oxide/zinc oxide (MBs-AO/GO/ZnO) membrane-based arrayed screen-printed electrodes (SPEs). The morphology of membranes was characterized by using a scanning probe microscope (SPM) and a field-emission scanning electron microscope (FE-SEM). The sensing characteristics were analyzed via the voltage-time (V-T) measurement system. The potentiometric arrayed AA biosensor showed the exceptional average sensitivity of 70.68 mV/decade over a wide linear range of AA concentration (7.8125 μM-2 mM), the short response time of 25 s, the lower limit of detection (LOD) of 0.04 μM, and the excellent selectivity. Furthermore, we investigated other analytical parameters of the potentiometric arrayed AA biosensor, such as the temperature effects, the lifetime, and the average sensitivity under microfluidic flow. The optimal average sensitivity of the biosensor integrated with the microfluidic framework was 72.21 mV/decade under microfluidic flow. Finally, the biosensor was applied to the remote AA detection by using the wireless sensing system. The results indicated that the average sensitivity of the potentiometric arrayed AA biosensor based on MBs-AO/GO/ZnO was 77.38 mV/decade during the monitoring in a long distance.

INDEX TERMS Zinc oxide (ZnO), graphene oxide (GO), magnetic beads (MBs), ascorbic acid (AA), screen-printed electrodes (SPEs), remote monitoring.

I. INTRODUCTION

Ascorbic acid (AA), is usually known as vitamin C, presents in many fruits and vegetables [1]. The normal AA level is from 0.007 mM (0.12 mg/dL) to 0.125 mM (2.20 mg/dL) for an adult [2]. And the maximum AA saturation concentration is 0.034 mM (0.60 mg/dL) for an adult; the over-consumption for vitamin C may result in urinary stones or diarrhea [3]. By the contrary, the severe deficiency of AA leads to scurvy [4]. Because the accurate AA detection is important for clinical diagnostics and food safety, a variety of biosensors for detection of AA have rapidly developed all over the worlds in recent years [5], [6].

Zinc oxide (ZnO), a wide bandgap (3.37 eV) semiconductor, has captivated a great deal of attention in a great deal of applications, such as piezoelectric devices [7], gas sensors [8], and dye-sensitized solar cells [9] because of its charge transfer properties, high isoelectric point (9.5), biocompatibility, chemical stability, and nontoxicity [10]. In addition, ZnO films can be processed on potentiometric substrates at low temperature so that they have been applied to many potentiometric electronics [11], [12]. In recent years, many biosensors are operated in amperometric or conductometric mode for AA detection [10], [13]–[15], but the reports

The associate editor coordinating the review of this manuscript and approving it for publication was Karol Malecha.

related to biosensors in potentiometric mode and applied screen-printed arrayed electrodes (SPEs) on a plastic substrate are rare. Hence, a sensitive potentiometric arrayed AA biosensor using arrayed SPEs has been exploited in this work.

Graphene oxide (GO), is obtained by oxidation of graphene, is a water-dispersible graphene derivative [16]. Because of GO with abundant oxygen-containing functional groups (hydroxyl, carbonyl, and carboxyl groups), the high specific surface area, and its unique $\pi - \pi$ stacking structure, GO can effectively enhance the enzyme immobilization [17], [18]. These functional groups provide GO an ability which adsorbs the ions in the solution [19]; it is conducive to improve the performance of a potentiometric biosensor. Besides, the charge transfer ability of membranes can be effectively improved owing to the excellent electrocatalytic activity [20].

Magnetic beads (MBs) are a type of non-toxic magnetic particles [21]. Their high specific surface area provides an appropriate microenvironment for enzymes, can maintain the high activity of enzymes and enhance the enzyme immobilization (easily connect with biomolecules), thereby improving the catalytic reaction velocity of a sensing membrane [22]–[24].

In this work, the sensing membranes were characterized by using a scanning probe microscope (SPM) and a field-emission scanning electron microscope (FE-SEM) firstly. Next, we investigated that the analytical performances of the potentiometric arrayed AA biosensor in the range of AA concentration from the concentration of scurvy (0.007 mM, 0.12 mg/dL) to the concentration of high-vitamin C (2 mM, 35.22 mg/dL), including sensitivity, response time, LOD, selectivity, temperature effects, and lifetime. Very recently, microfluidics has been applied to a lot of analyses of sensing characteristics because it provides short response time and reduces wastage of reagent [25], [26]. In order to keep up with this unavoidable trend, the sensitivity and linearity of the potentiometric arrayed AA biosensor under microfluidic flow have been analyzed in this work. In, addition, remote detection also has come into the research focus [27], [29]. Therefore, an XBee module based on the ZigBee standard was applied to realizing the AA detection in a long distance.

II. EXPERIMEANTAL

A. FABRICATION OF POTENTIOMETRIC ARRAYED AA BIOSENSOR

In our previous study [30]–[32], the detailed information of chemicals can be found, and more details of the fabrication process are illustrated. All chemicals used in this work were of analytical grade and used without further purification. Apart from this, the ZnO (99.99% purity) target, was purchased from Ultimate Material Technology Co., Ltd. (Taiwan), was used to deposit the sensing membranes on a polyethylene terephthalate (PET) substrate. The process steps were simply described as follows:

(1) A PET substrate (Dimension: 3 cm × 3.5 cm) was cleaned by the standard preprocesses.

(2) The silver arrayed electrodes were printed onto a PET substrate by using screen-printing technology.

(3) ZnO membranes were deposited on a PET substrate via the radio frequency (RF) vacuum sputtering system; the deposition parameters are shown in Table 1.

TABLE 1. The deposition parameters for ZnO membrane via the RF vacuum sputtering system.

Material	ZnO
Deposition pressure (Torr)	3×10^{-3}
Duration (min)	30
Substrate temperature (°C)	25
Gas flow (Ar : O_2, sccm)	9:1
RF power (W)	60

(4) Epoxy was used to determine the sensing area of windows and protect silver conductive wires from a solution (Dimension: 1.77 mm^2).

(5) According to the optimal parameter of GO solution [30], the 0.3 wt% GO solution was used to modify ZnO membranes by using the drop-coating method.

(6) The cross-linker (3-glycidoxypropyl-trimethoxysilane (GPTS): toluene, vol. ratio: 1:4) were dropped on ZnO/GO membranes to effectively connect enzymes with a carrier.

(7) According to the optimal ratio of the enzymatic solution (MBs: ascorbate oxidase (AO), vol. ratio: 1:1) [31], the MBs-AO solution was immobilized on GO/ZnO membranes.

(8) After complete the enzyme immobilization, the potentiometric arrayed AA biosensor based on MBs-AO/GO/ZnO was stored in a refrigerator at 25° when not in use.

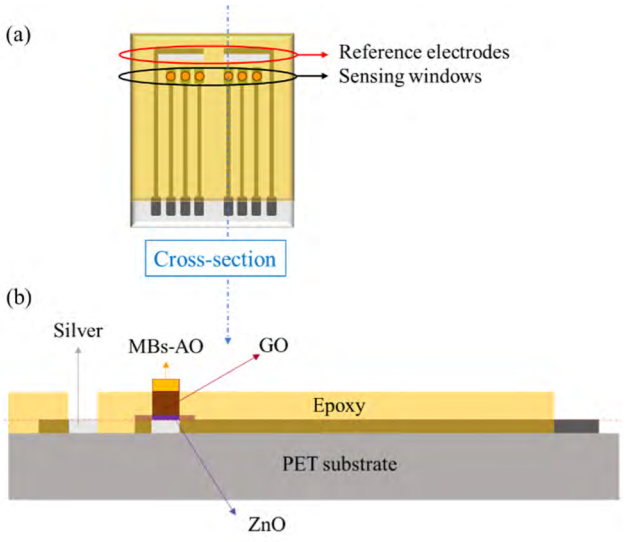

FIGURE 1. The schematic diagrams of the potentiometric arrayed AA biosensor based on MBs-AO/GO/ZnO. (a) top view and (b) cross-section.

After following the process steps, the biosensor was fabricated successfully. The schematic diagrams of the potentiometric arrayed AA biosensor based on MBs-AO/GO/ZnO are shown in Fig. 1. The functions of each layer are addressed as follows: Silver acts as the reference electrodes and conductive

wires. ZnO is used as a basic sensing matrix. GO can increase a large number of surface active sites owing to the abundant oxygen groups and the layer structure, can enhance the sensing characteristics. MBs provide the high surface-volume ratio for the immobilization of enzymes increasing the enzyme loading on a membrane. AO is used as the biometric layer, catalyzes AA and can prevent the noises of other interfering substances, is the main reaction layer of the potentiometric arrayed AA biosensor.

B. POTENTIOMETRIC MEASUREMENT SYSTEM

In this work, we used two types of measurement systems to characterize the analytical performances of a biosensor. The voltage-time (V-T) measurement was used to measure most of the sensing parameters. After determining the sensing parameters, the wireless sensing system was applied to the remote monitoring for the AA detection further. Two types of measurements are described as follows:

The V-T measurement system was composed of a power supply, a readout circuit, a data acquisition card (DAQ card, Model: NI USB-6201, National Instrument Corp., U.S.A.), and a computer with the LabVIEW program [33]. The readout circuit consists of the six instrumentation amplifiers (LT1167, Analog Devices, Inc., U.S.A.). In terms of the signal communication, the signals were sent to the DAQ card to intercept the bioelectronic signal and convert the analog signals into the digital signals, then the signals were processed through a computer with the LabVIEW program.

The wireless sensing system was composed of a set of XBee module, an Arduino Mega 2560, a readout circuit, a power supply, and a computer with the LabVIEW program [34]. A set of XBee module included a router and a coordinator, they were used as the transmitter and the receiver, respectively. The readout circuit was composed of the six instrumentation amplifiers (AD623, Analog Devices, Inc., U.S.A.). The Arduino Mega 2560 (Atmel Corporation, U.S.A.), is the microcontroller board based on the ATmega 2560, which is supplied to the XBee router and the readout circuit, respectively. In terms of the signal communication, through controlling of the Arduino Mega 2560, the XBee router received the measurement signals and wirelessly sent the measurement signals to the XBee coordinator, and the signals were transmitted to a computer with the LabVIEW program.

The measurement systems have been reported in our previous work [33], [34]; the measuring principle for potentiometric biosensors via both measurement systems was explained in detail. In addition, the photo in realistic measurement is shown in Fig. 2, which the biosensor was measured via the wireless sensing system.

C. MICROFLUIDIC FRAMEWORK

According to the previous investigation [35], the microfluidic device was fabricated by using polydimethylsiloxane (PDMS) and curing agents. The 2D pattern of the microfluidic channel is shown in Fig. 3 [35, Fig. 4(b)], and

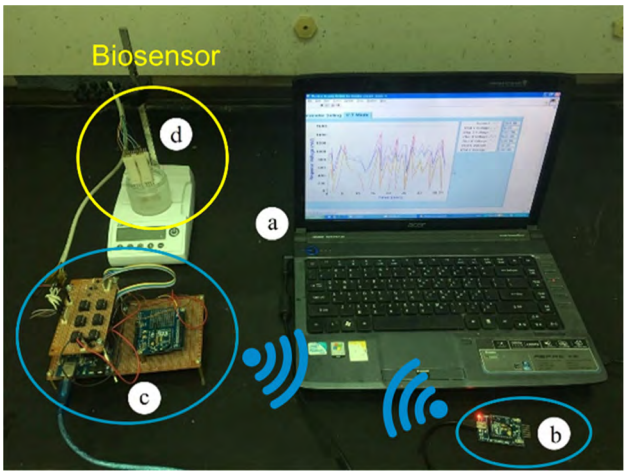

FIGURE 2. The photo in realistic measurement which the biosensor was measured via the wireless sensing system. (a) a computer with the LabVIEW program, (b) a receiver of an XBee module, (c) a readout circuit integrated with an Arduino Mega 2560 and a transmitter of an XBee module, (d) a biosensor and a test solution.

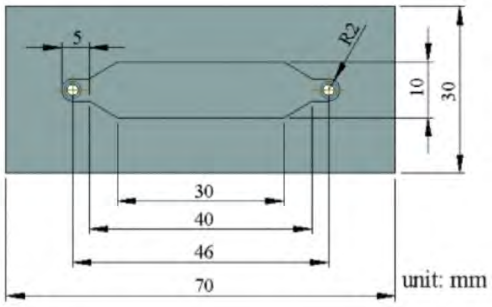

FIGURE 3. The 2D pattern of the microfluidic channel [35].

the height is 25 μm. The two acrylic sheets were used to fix a potentiometric arrayed AA biosensor and the microfluidic device (sandwich structure), as shown in Fig. 4(b). Next, they were respectively integrated with a pump and an injector via pipes and with the V-T measurement system via conductive wires. The schematic diagram of the microfluidic framework is shown in Fig. 4. During measurement, the test solution was pumped through the microfluidic channel by an injector and a pump. Subsequently, the flow rate was controlled by a pump. The average sensitivity and linearity of a biosensor at different flow rates of microfluidic flow was analyzed in this work.

D. INSTRUMENTS

The RF vacuum sputtering system was used to deposit ZnO membranes. The semi-automatic screen printer (Model: HJ-55AC, Taiwan), which was used to print arrayed electrodes and encapsulation, was purchased from Houn Jien Co., Ltd. The thermostatic water bath and the temperature controller (Model: TAIE FY-400, Taiwan) were used to investigate the temperature effects of biosensors, were purchased from Taiwan Instrument & Control Co., Ltd.

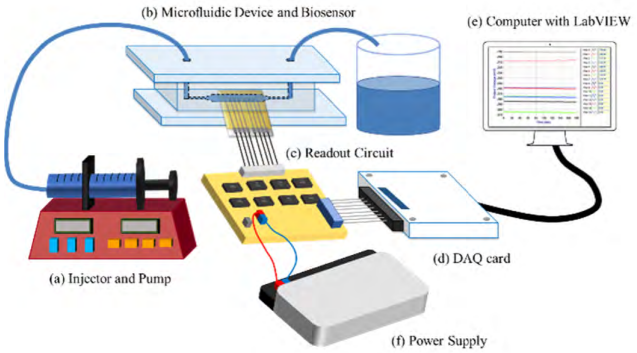

FIGURE 4. The schematic diagram of the microfluidic framework when a biosensor is being measured.

The FE-SEM equipped with an energy dispersive X-ray spectrometry (EDS) detector (Model: JSM-6701F, Japan) was used to investigate the morphology and elemental analysis of membranes, was purchased from JEOL Ltd. The SPM (Model: Dimension Icon, U.S.A) was used to examine the surface roughness of membranes, was purchased from Bruker Corp.

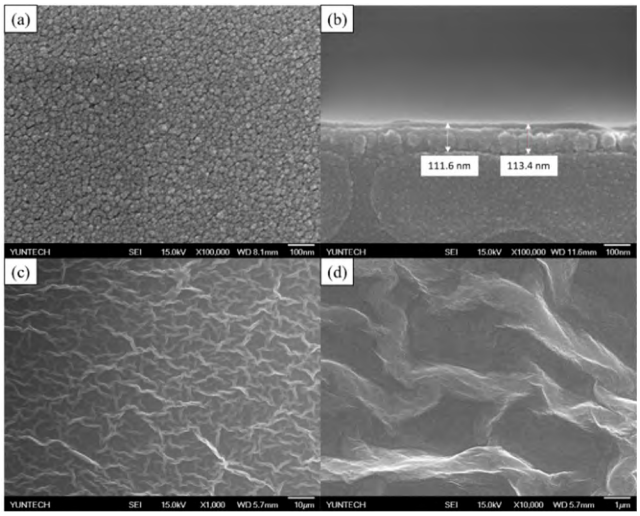

FIGURE 5. The FE-SEM (a) top view and (b) cross-section images of the ZnO membrane. The FE-SEM top view images of the GO membrane in (c) 1k and (d) 10k magnification.

III. RESULTS AND DISCUSSION

A. MORPHOLOGY AND SURFACE ROUGHNESS OF MEMBRANES

The ZnO membrane was deposited on a Si substrate, and the FE-SEM images are shown in Fig. 5(a-b). The top view of the ZnO membrane showed granular and compact. The thickness is 109.2±5.0 nm (10 sampling points). Apart from this, the FE-SEM top view images of GO membrane were shot in different magnifications, as shown in Fig. 5(c-d). The surface morphology exhibited a crumpled structure because GO sheets were intensely folded and stacked.

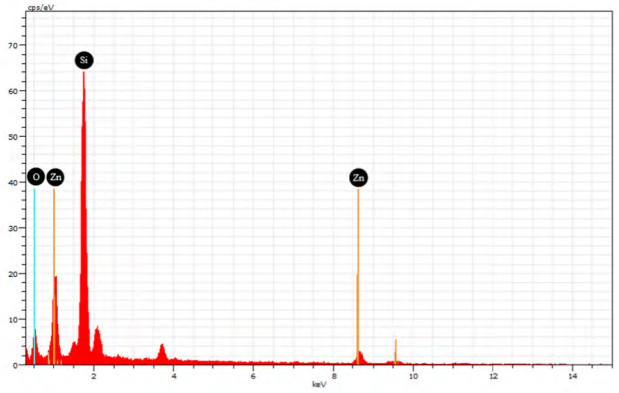

FIGURE 6. The EDS spectrum of the ZnO membrane on a Si substrate.

As shown in Fig. 6, the EDS spectrum showed that obvious Zn, O, and Si peaks could be observed. The Si peak was originated from a Si substrate. The EDS results were in accordance with expectations.

The surface roughness of the membranes was examined via SPM, including ZnO, GO/ZnO and MBs/GO/ZnO membranes. The image projected surface area was set as 2500 μm^2 (50μm × 50μm) to analyze roughness of films on the large area. The morphologies of different membranes are shown in Fig. 7. ZnO showed a platform as shown in Fig. 7(a); GO/ZnO was flake as well as showing large peaks and valleys as shown in Fig. 7(b); MBs/GO/ZnO exhibited more intensively small peaks and valleys as shown in Fig. 7(c). Image R_q is the root mean square average of height deviations measured from the mean data plane [36]. The image R_q were 67.5 nm, 117 nm, and 316 nm for ZnO, GO/ZnO, and MBs/GO/ZnO, respectively. The surface roughness analysis exhibited that the image R_q of MBs/GO/ZnO was increased obviously. The surface roughness of the membranes is enhanced efficiently. The roughness of membrane is usually related to electrochemical reaction, enzyme loading, and the electrocatalytic activity of the electrode; the increment of the surface roughness can enhance the sensing properties of a biosensor [37], [38].

B. AVERAGE SENSITIVITY AND LINEARITY

The sensing mechanism of the potentiometric arrayed AA biosensor is based on an enzymatic reaction catalyzed by AO, as shown follows [39], [40]:

$$\text{Ascorbic acid} \xrightarrow{\text{Ascorbate oxidase}} \text{Dehydro} - \text{L} - \text{ascorbic acid} + 2\text{H}^+ + 2\text{e}^- \quad (1)$$

From the formula (1), AA will be converted into dehydro-L-ascorbic acid, hydrogen ions (H^+) and electrons. Because AA is catalyzed in high rate by AO, the produced H^+ will affect the pH value in the micro-surrounding of the sensing electrode. The surface potential of the sensing electrode is changed further owing to the micro-variation of the pH value. According to the Nernst equation and our previous

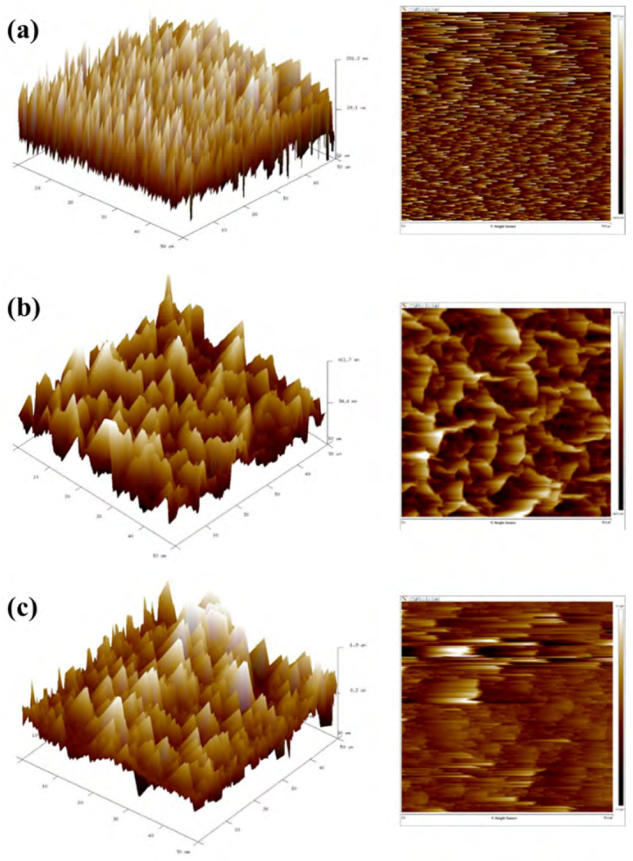

FIGURE 7. The surface morphology of the (a) ZnO, (b) GO/ZnO, and (c) MBs/GO/ZnO membranes via SPM.

study [32], [41], the sensing mechanism can follow the equation (2).

$$\frac{\partial E}{\partial pH} = 2.303\frac{RT}{F} \tag{2}$$

where E is the electromotive force (EMF), E^0 is the standard potential of the reference electrode, R is the gas constant, T is the temperature in Kelvins, F is the Faraday's constant, and pH is the pH of the electrolyte.

The potentiometric arrayed AA biosensor based on MBs-AO/GO/ZnO was immersed in 50 mM PBS solutions (pH 7.0) over an AA concentration (7.8125 μM-2 mM), and then the data were recorded via the V-T measurement system. The average response voltages (mean) and the error bars (standard deviation, SD) were obtained from the response voltages of the six windows (1.77 mm^2 per window). According to the obtained data, the average sensitivity and linearity were calculated by Origin 7.0. The potential response curves are shown in Fig. 8. The average sensitivity and linearity of the potentiometric arrayed AA biosensor based on MBs-AO/GO/ZnO were 70.68 mV/decade and 0.996, respectively.

C. RESPONSE TIME

Response time is the period of time that achieve 95% of the steady state voltage from the origin state voltage over the

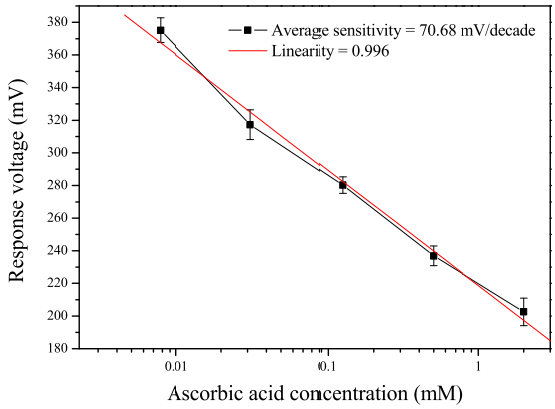

FIGURE 8. The response characteristics of the potentiometric arrayed AA biosensor based on MBs-AO/GO/ZnO over an AA concentration (7.8125 μM-2 mM) via the V-T measurement system.

whole concentration range [23]. Origin state can be defined as a baseline, which is the output voltage measured that the biosensor is immersed in a buffer solution without any analytes [42]. Steady state is the output voltage that the biosensor is in a buffer solution with analytes. In this study, the potentiometric arrayed AA biosensor based on MBs-AO/GO/ZnO was immersed in a pure 50 mM PBS (pH 7.0) solution, and the response voltage maintained the steady state for 30 s. Next, AA added into a pure 50 mM PBS solution (PBS solution with 0.125 mM AA concentration) to observe the response voltages of the biosensor.

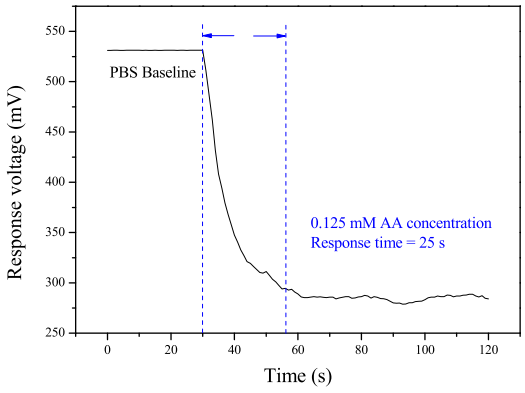

FIGURE 9. The response curve of the potentiometric arrayed AA biosensor based on MBs-AO/GO/ZnO was immersed in a PBS solution (pH 7.0) after achieving 0.125 mM AA concentration.

According to the definition, its response time is the period of time of the response voltage between the origin state and the 95% steady state. As shown in Fig. 9, the potentiometric arrayed AA biosensor based on MBs-AO/GO/ZnO exhibited the low response time of 25 s.

D. LIMIT OF DETECTION

Limit of detection (LOD) is defined as the lowest concentration of analytes in a sample that can be detected, not quantitated. It is expressed as a concentration at a specified

signal-to-noise ratio, the ratio is usually three-to-one (S/N = 3) following the equations (3 and 4) [43]:

$$\mathrm{LOD} = 3\sigma/\mathrm{S}_0 \tag{3}$$

$$\sigma = \sqrt{\frac{\sum |x - \bar{x}|^2}{n}} \tag{4}$$

where LOD is the limit of detection, S_0 is the sensitivity, σ is the standard deviation, Σ means the sum, x is a value in the data set, $\bar{x}$ is the mean of the data set, and n is the number of data points.

The response voltages of the potentiometric arrayed AA biosensor based on MBs-AO/GO/ZnO were measured in a pure 50 mM PBS solution (pH 7.0) via the V-T measurement system, and the measurements were repeated for 7 times (N = 7). Next, the mean of the response voltages was as the baseline and the standard deviations (σ) were calculated. The results were: S_0 was 70.68 mV/decade, $\bar{x}$ was 531.13 mV, and σ was 9.75×10^{-2} mV. Finally, the LOD was obtained according to the equations (3 and 4). The potentiometric arrayed AA biosensor based on MBs-AO/GO/ZnO performed the low LOD of 0.04 μM.

E. SELECTIVITY

Glucose and uric acid (UA) possibly introduce some noises, thereby the affecting response of a potentiometric AA biosensor [44], [45]. In addition, the interfering substances in amperometric mode were also used for the test of selectivity, such as urea [46]. Thus, the common interfering substances in human blood were used to examine the selectivity of the potentiometric arrayed AA biosensors, including glucose, urea, and UA. For experimental details, the AA biosensor was immersed in a 50 mM PBS solution with 0.06 mM AA concentration until the response voltage maintained equilibrium. After that, glucose, urea, and UA were sequentially added into a PBS solution per 60 s. Finally, the AA concentration was increased to 0.125 mM (the saturation concentration in human blood) in order to demonstrate the specificity of the biosensors.

As shown in Fig. 10, these interfering substances have no influence on the response voltage. In other words, the results indicated the exceptional specificity of AO toward AA. The potentiometric arrayed AA biosensor based on MBs-AO/GO/ZnO displayed the excellent selectivity.

F. TEMPERATURE EFFECTS

In order to carry out the temperature effects, the thermostatic water bath and the temperature controller were used to control and maintain the temperature of the water bath, and then the test solutions and biosensor were placed in the thermostatic water bath. The temperature range was from 25 °C (room temperature) to 65 °C. The biosensor was measured in 50 mM PBS solutions (pH 7.0) over an AA concentration (7.8125 μM-2 mM) and within a temperature range from 25 °C to 65 °C via the V-T measurement system.

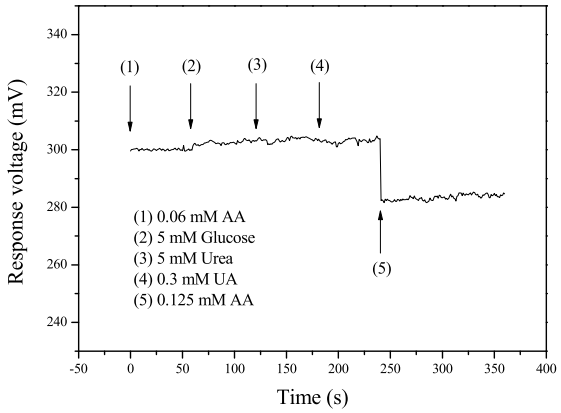

FIGURE 10. The selectivity of the potentiometric arrayed AA biosensor based on MBs-AO/GO/ZnO under the presence of other interference substances.

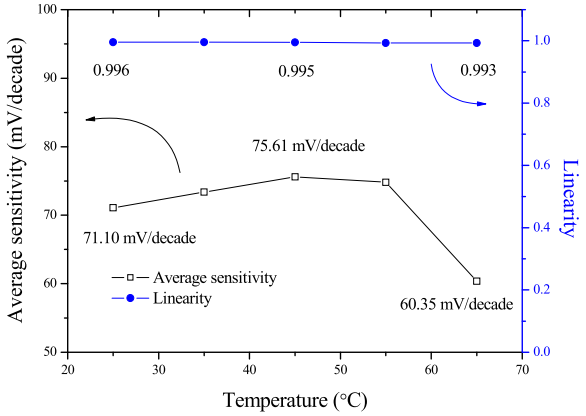

FIGURE 11. The temperature effects of the potentiometric arrayed AA biosensor based on MBs-AO/GO/ZnO.

TABLE 2. The average sensitivity and linearity of the potentiometric arrayed AA biosensor based on MBs-AO/GO/ZnO at different temperatures.

Temperature (°C)	Average sensitivity (mV/mM)	Linearity
25	71.10	0.996
35	73.37	0.996
45	75.61	0.995
55	74.81	0.993
65	60.35	0.993

As shown in Fig. 11 and Table 2, the average sensitivities of the biosensors based on MBs-AO/GO/ZnO increased continuously within the temperature range from 25 °C to 45 °C; the average sensitivity for MBs-AO/GO/ZnO was increased from 71.10 mV/decade to 75.61 mV/decade. Temperature is a factor for the sensitivity of a potentiometric biosensor according to the Nernst equation. Because the raised temperature, the sensitivity of the AA biosensors was increased accordingly. Furthermore, the activity of an enzymatic membrane will influence the sensitivity of a biosensor when the temperature is changed. The average sensitivity of the biosensor based

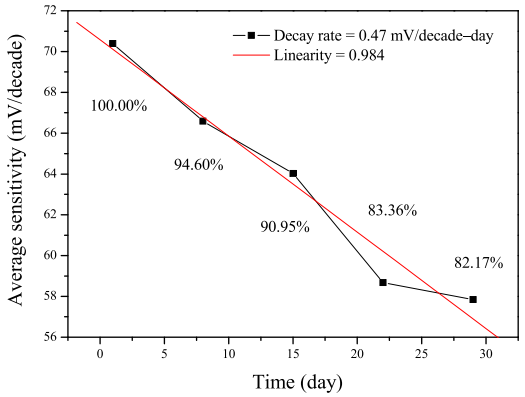

FIGURE 12. The decay rate of the potentiometric arrayed AA biosensor based on MBs-AO/GO/ZnO within 29 days.

TABLE 3. The relative average sensitivity (S) of the potentiometric arrayed AA biosensors measured on the different time.

Membrane	Time (day)	S_{test} (mV/decade)	S (%)
MBs-AO/GO/ZnO	1	70.39 ($S_{initial}$)	100.00
	8	66.59	94.60
	15	64.02	90.95
	22	58.68	83.36
	29	57.84	82.17

on MBs-AO/GO/ZnO decreased from 75.61 mV/decade to 60.35 mV/decade. As shown in Table 2, the average sensitivity of the biosensor merely had a little decrement within the temperature range from 45 °C to 55 °C. However, the average sensitivity was dropped significantly when the temperature was increased to 65 °C. Based on the previous study [47], the maximal activity of the AO is 50 °C. AO will enter denaturation once the temperature exceeds 60 °C. As a consequence, the average sensitivities of the AA biosensors had a tremendous drop at 65 °C. Besides, J. C. B. Fernandes *et al.* [46] analyzed the response of the potentiometric biosensor based on AO within the range from 25 °C to 50 °C. The results indicated that the best response of the biosensor was obtained at higher temperature. Kannouji *et al.* [48] investigated the thermal stability of the immobilized AO on a polycarbonate (PC) strip at different temperatures from 40 °C to 70 °C. The immobilized AO retained about 75% residual activity at 50 °C. These studies showed that the sensitivity depended on the activity of AO. According to the results, the biosensor was suitable for a temperature range from 25 °C to 55 °C for the determination of AA.

G. LIFETIME AND DECAY RATE

Most biosensors have a certain lifetime because of a critical drawback, which the biological materials usually have a fairly limited lifetime [49]. In general, biosensors are tested their lifetime in different storage time under identical conditions. Lifetime is defined as the storage or operational time necessary for the decreased sensitivity to 90% within the linear concentration range [50]. In this study, the measuring time for the lifetime was 29 days. The average sensitivities of the

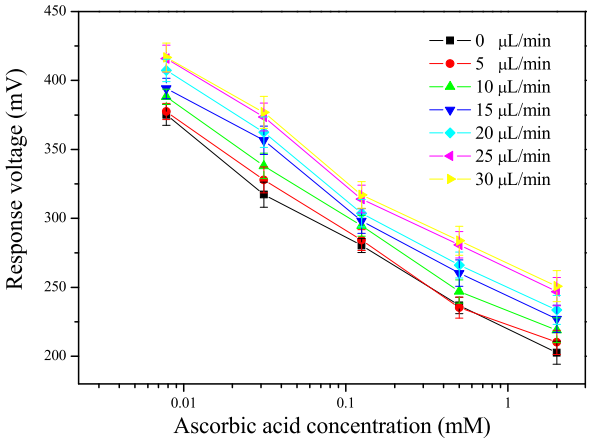

FIGURE 13. The response characteristics of the potentiometric arrayed AA biosensor based on MBs-AO/GO/ZnO over an AA concentration (7.8125μM-2 mM) and at flow rates from 0 μL/min to 30 μL/min.

TABLE 4. The average sensitivity and linearity of the potentiometric arrayed AA biosensor based on MBs-AO/GO/ZnO over an AA concentration (7.8125 μM-2 mM) and at flow rates from 0 μL/min to 30 μL/min.

Membrane	Flow rate (μL/min)	Average sensitivity (mV/decade)	Linearity
MBs-AO/GO/ZnO	0	70.68	0.996
	5	70.95	0.995
	10	71.38	0.996
	15	71.50	0.995
	20	72.21	0.995
	25	71.54	0.994
	30	71.21	0.993

biosensor were recorded at room temperature every 7 days, and the biosensor was stored in a refrigerator at 4 °C when not in used. After that, the relative average sensitivity (S) were determined according to the equation (5). The equation (5) is shown as follows:

$$S = \frac{S_{test}}{S_{initial}} \tag{5}$$

where S is the relative average sensitivity, S_{test} is the average sensitivity measured on the different time, $S_{initial}$ is the initial average sensitivity. The S was continuously measured on the different dates until the S was decreased to 90%; this period of time is the lifetime of a biosensor. Furthermore, the decay rate (average sensitivity vs. time) was calculated by using Origin 7.0. The data measured on the different time are shown in Fig. 12 and Table 3. As shown in Fig. 12, the decay rate of the potentiometric arrayed AA biosensor based MBs-AO/GO/ZnO was 0.47 mV/decade-day. The relative average sensitivities maintained above 80% within 29 days. It could be proven that the potentiometric arrayed AA biosensor possess the stability in used for a long period.

H. SENSING CHARACTERISTICS UNDER DYNAMIC MICROFLUIDIC FLOW

All experiment details were as similar as Section B. In order to analyze the average sensitivities under dynamic

TABLE 5. The potentiometric AA biosensors based on different electrodes [44], [45], [51]–[54].

Electrode	Linear range	Sensitivity	Linearity	Response time	LOD	Ref.
MBs-AO/GO/ZnO/Ag	7.8125 μM-2 mM	70.68 mV/decade	0.996	25 s	0.04 μM	In this study
MIP-Au	1 μM-0.1 mM	213 mV/decade	0.993	N/A	0.01 μM	[44] 2018
NanoCoPc/GCE	50 μM-55 mM	60.8 mV/decade	N/A	< 15 s	0.1 μM	[45] 2005
PPy-MIPox/GCE	5 μM-2 mM	57 mV/decade	0.990	4-5 min	3 μM	[51] 2011
PANI-CSA	0.32 mM-5.62 mM	25.91 mV/decade	N/A	N/A	0.05 mM	[52] 2007
Ionophore/PVC/CTR/Ag	0.02 mM-2 mM	49.3 mV/decade	N/A	5 min	N/A	[53] 2004
AO/ZnO NRs/Au	1 μM-50 mM	32 mV/decade	N/A	< 10 s	1 μM	[54] 2011

Note: MBs: magnetic beads; GO: graphene oxide; MIP: molecularly imprinted polymer; NanoCoPc: cobalt phthalocyanine nanoparticle; GCE: glassy carbon electrode; PPy: polypyrrole; MIPox: oxidation molecularly imprinted polymer; PANI: polyaniline; CSA: camphor sulfonic acid; PVC: polyvinyl chloride; CTR: conductive thermoplastic resin; NRs: nanorods

microfluidic flow, the potentiometric arrayed AA biosensor was placed in the microfluidic device. Subsequently, the test solution was injected into the microfluidic channel by a pump and an injector. The flow rates were set as a range of 0 μL/min-30 μL/min. As shown in Fig. 13 and Table 4, the best average sensitivity of the potentiometric arrayed AA biosensor based on MBs-AO/GO/ZnO was 72.21 mV/decade at the flow rate of 20 μL/min. The results indicated that the average sensitivities under microfluidic flow were better than under the static microfluid. In the previous study by the same research group [32], the optimal average sensitivity of the AA biosensor MBs-AO/GO/IGZO/Al was 81.7 mV/decade at the flow rate of 25 μL/min. The results were in accordance with the previous study, the optimal flow rate was still within a range of 15 μL/min to 25 μL/min.

I. REMOTE MONITORING

In order to realize the remote monitoring, the potentiometric arrayed AA biosensor based on MBs-AO/GO/ZnO was measured via the wireless sensing system. As shown in Fig. 14, the results indicated that the average sensitivity and linearity were similar to Fig. 8 (via the V-T measurement system). The large error bars were due to the different measurement systems. In terms of the difference in both the measurement systems using the different analog-to-digital converters, the Arduino Mega 2560 of the wireless sensing system was used instead of the NI DAQ card of the potentiometric measurement system. The resolutions of Arduino Mega 2560 and NI DAQ card are respectively denoted 10 bits and 16 bits. Based on the reason, the errors of the wireless sensing system were larger than them of the V-T measurement system. The reliability of the wireless sensing system was also excellent although the standard deviations of this system were larger than them of the V-T measurement system. In this study, the average sensitivity and linearity of the potentiometric arrayed AA biosensor based on MBs-AO/GO/ZnO were 77.38 mV/decade and 0.990, respectively.

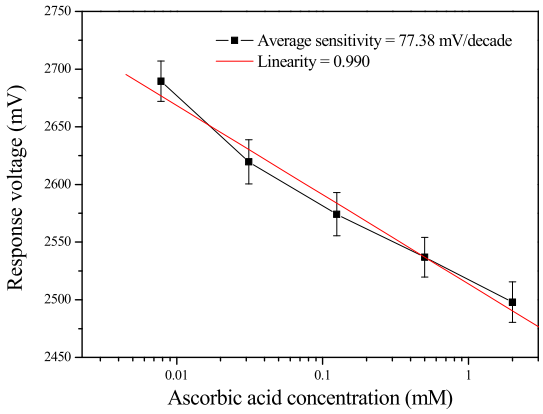

FIGURE 14. The response characteristics of the potentiometric arrayed AA biosensor based on MBs-AO/GO/ZnO over an AA concentration (7.8125 μ M-2 mM) via the wireless sensing system.

J. COMPARISONS OF AA BIOSENSORS

The comparison of different potentiometric AA biosensors in recent years are summarized in Table 5 [44], [45], [51]–[54]. In this study, the potentiometric arrayed AA biosensor based on MBs-AO/GO/ZnO showed the average sensitivity of 70.68 mV/decade and the linearity of 0.996 over a wide AA concentration range (7.8125 μM-2 mM). The sensitivity has been higher than most AA biosensors. In addition to the

exceptional average sensitivity, the biosensors had the fast response time (25 s) and the low LOD (0.04 μM). The results showed that this structure of the biosensor will be promising for the determination of AA.

IV. CONCLUSION

The sensitive potentiometric AA biosensor using MBs-AO/GO/ZnO membranes-based arrayed SPEs has proposed in this work. A variety of analytical performances of the biosensor were characterized, including the remarkable sensitivity of 70.68 mV/decade over a wide range of AA concentration (7.8125 μM-2 mM), the short response time of 25 s, the low LOD of 0.04 μM, the good selectivity, the suitable range of temperature from 25 °C to 55 °C, the long storage stability, and the optimal sensitivity of 72.21 mV/decade at the flow rate of 20 μL/min. The analytical performances of this biosensor are better than most of the potentiometric AA biosensors in recent years, and the facile fabrication processes provides a promising method for potentiometric biosensors. Furthermore, the reported biosensor was successfully applied to the remote monitoring for AA. By applying the wireless sensing system, the average sensitivity and linearity of the potentiometric arrayed AA biosensor based on MBs-AO/GO/ZnO were 77.38 mV/decade and 0.990, respectively.

REFERENCES

[1] Z. Gazdik, O. Zitka, J. Petrlova, V. Adam, J. Zehnalek, A. Horna, V. Reznicek, M. Beklova, and R. Kizek, "Determination of vitamin C (ascorbic acid) using high performance liquid chromatography coupled with electrochemical detection," *Sensors*, vol. 8, pp. 7097–7112, Nov. 2008.

[2] M. Noroozifar, M. Khorasani-Motlagh, R. Akbari, and M. B. Parizi, "Simultaneous voltammetric measurement of ascorbic acid, epinephrine, uric acid and tyrosine at aglassy carbon electrode modified with nanozeolite-multiwall carbon nanotube," *Anal. Bioanal. Chem. Res.*, vol. 1, pp. 62–72, Jun. 2014.

[3] H. Liu, W. Na, Z. Liu, X. Chen, and X. Su, "A novel turn-on fluorescent strategy for sensing ascorbic acid using graphene quantum dots as fluorescent probe," *Biosens. Bioelectron.*, vol. 92, pp. 229–233, Jun. 2017.

[4] Y. G. Lee, B. X. Liao, and Y. C. Weng, "Ruthenium oxide modified nickel electrode for ascorbic acid detection," *Chemosphere*, vol. 173, pp. 512–519, Apr. 2017.

[5] N. Arumugam and J. Kim, "Quantum dots attached to graphene oxide for sensitive detection of ascorbic acid in aqueous solutions," *Mater. Sci. Eng. C*, vol. 92, pp. 720–725, Nov. 2018.

[6] R. Sha and S. Badhulika, "Facile green synthesis of reduced graphene oxide/tin oxide composite for highly selective and ultra-sensitive detection of ascorbic acid," *J. Electroanal. Chem.*, vol. 816, pp. 30–37, May 2018.

[7] M. S. Al-Ruqeishi, T. Mohiuddin, B. Al-Habsi, F. Al-Ruqeishi, A. Al-Fahdi, and A. Al-Khusaibi, "Piezoelectric nanogenerator based on ZnO nanorods," *Arab. J. Chem.*, Dec. 2016. doi: 10.1016/j.arabjc.2016.12.010.

[8] L. Zhu and W. Zeng, "Room-temperature gas sensing of ZnO-based gas sensor: A review," *Sens. Actuators A, Phys.*, vol. 267, pp. 242–261, Nov. 2017.

[9] M.-H. Jung, "High efficiency dye-sensitized solar cells based on the ZnO nanoparticle aggregation sphere," *Mater. Chem. Phys.*, vol. 202, pp. 234–244, Dec. 2017.

[10] S. K. Arya, S. Saha, J. E. Ramirez-Vick, V. Gupta, S. Bhansali, and S. P. Singh, "Recent advances in ZnO nanostructures and thin films for biosensor applications: Review," *Anal. Chim. Acta*, vol. 737, pp. 1–21, Aug. 2012.

[11] J. W. Kang, W. I. Jeong, J. J. Kim, H. K. Kim, D. G. Kim, and G. H. Lee, "High-performance potentiometric organic light-emitting diodes using amorphous indium zinc oxide anode," *Electrochem. Solid-State Lett.*, vol. 10, no. 6, pp. J75–J78, Mar. 2007. doi: 10.1149/1.2720635.

[12] Y.-H. Zhang, Z.-X. Mei, H.-L. Liang, and X.-L. Du, "Review of flexible and transparent thin-film transistors based on zinc oxide and related materials," *Chin. Phys. B*, vol. 26, Jan. 2017, Art. no. 047307.

[13] C. Singhal, N. Malhotra, C. S. Pundir, Deepshikha, and J. Narang, "An enzyme free Vitamin C augmented sensing with different ZnO morphologies on SnO_2/F transparent glass electrode: A comparative study," *Mater. Sci. Eng. C*, vol. 69, pp. 769–779, Dec. 2016.

[14] S. A. Kumar, H.-W. Cheng, and S.-M. Chen, "Electroanalysis of ascorbic acid (vitamin C) using nano-ZnO/poly(luminol) hybrid film modified electrode," *Reactive Funct. Polym.*, vol. 69, pp. 364–370, Jun. 2009.

[15] A. Mahmoud, M. Echabaane, K. Omri, L. El Mir, and R. Ben Chaabane, "Development of an impedimetric non enzymatic sensor based on ZnO and Cu doped ZnO nanoparticles for the detection of glucose," *J. Alloys Compounds*, vol. 786, pp. 960–968, May 2019.

[16] D. Li, M. B. Müller, S. Gilje, R. B. Kaner, and G. G. Wallace, "Processable aqueous dispersions of graphene nanosheets," *Nature Nanotechnol.*, vol. 3, pp. 101–105, Jan. 2009.

[17] C. I. L. Justino, A. R. Gomes, A. C. Freitas, A. C. Duarte, and T. A. P. Rocha-Santos, "Graphene based sensors and biosensors," *Trends Anal. Chem.*, vol. 91, pp. 53–66, Jun. 2017.

[18] J. Zhang, F. Zhang, H. Yang, X. Huang, H. Liu, J. Zhang, and S. Guo, "Graphene oxide as a matrix for enzyme immobilization," *Langmuir*, vol. 26, pp. 6083–6085, Mar. 2010.

[19] S. Chowdhury and R. Balasubramanian, "Recent advances in the use of graphene-family nanoadsorbents for removal of toxic pollutants from wastewater," *Adv. Colloid Interface Sci.*, vol. 204, pp. 35–36, Feb. 2014.

[20] J. Lee, J. Kim, S. Kim, and D. H. Min, "Biosensors based on graphene oxide and its biomedical application," *Adv. Drug Del. Rev.*, vol. 105, pp. 275–287, Oct. 2016.

[21] A. Kumar, I. Y. Galaev, and B. Mattiasson, *Cell Separation: Fundamentals, Analytical and Preparative Methods*. Berlin, Germany: Springer, 2007, pp. 57–59.

[22] Y. Xianyu, Q. Wang, and Y. Chen, "Magnetic particles-enabled biosensors for point-of-care testing," *Trends Anal. Chem.*, vol. 106, pp. 213–224, Sep. 2018.

[23] K. Khun, Z. H. Ibupoto, J. Lu, M. S. Al Salhi, M. Atif, A. A. Ansari, and M. Willander, "Potentiometric glucose sensor based on the glucose oxidase immobilized iron ferrite magnetic particle/chitosan composite modified gold coated glass electrode," *Sens. Actuators B, Chem.*, vol. 173, pp. 698–703, Oct. 2012.

[24] S. Kiralp, A. Topcu, G. Bayramoglu, M. Y. Arica, and L. Toppare, "Alcohol determination via covalent enzyme immobilization on magnetic beads," *Sens. Actuators B, Chem.*, vol. 128, pp. 521–528, Jan. 2008.

[25] D. Xu, X. Huang, J. Guo, and X. Ma, "Automatic smartphone-based microfluidic biosensor system at the point of care," *Biosensors Bioelectron.*, vol. 110, pp. 78–88, Jul. 2018.

[26] J. F. C. Loo, A. H. P. Ho, A. P. F. Turner, and W. C. Mak, "Integrated printed microfluidic biosensors," *Trends Biotechnol.*, Apr. 2019. doi: 10.1016/j.tibtech.2019.03.009.

[27] S. Al-Sarawi, M. Anbar, K. Alieyan, and M. Alzubaidi, "Internet of Things (IoT) communication protocols: Review," in *Proc. ICIT*, Amman, Jordan, May 2017, pp. 685–690.

[28] Y.-H. Liao and J.-C. Chou, "Potentiometric multisensor based on ruthenium dioxide thin film with a Bluetooth wireless and Web-based remote measurement system," *IEEE Sensors J.*, vol. 9, no. 12, pp. 1887–1894, Dec. 2009.

[29] S.-J. Jung and W.-Y. Chung, "Non-intrusive healthcare system in global machine-to-machine networks," *IEEE Sensors J.*, vol. 13, no. 12, pp. 4824–4830, Dec. 2013.

[30] J.-C. Chou, Y.-X. Wu, Y.-H. Liao, C.-H. Lai, S.-J. Yan, C.-Y. Wu, Y.-H. Liao, C.-H. Lai, S.-J. Yan, C.-Y. Wu, and S.-H. Lin, "Flexible arrayed enzymatic l-ascorbic acid biosensor based on IGZO/Al membrane modified by graphene oxide," *IEEE Trans. Nano.*, vol. 17, no. 3, pp. 452–459, May 2018.

[31] J.-C. Chou, Y.-X. Wu, P.-Y. Kuo, C.-H. Lai, Y.-H. Nien, S.-H. Lin, S.-J. Yan, C.-Y. Wu, and Y.-H. Liao, "Improving the properties of L-ascorbic acid biosensor based on GO/IGZO/Al using magnetic beads," *IEEE Trans. Electron Devices*, vol. 66, no. 4, pp. 1924–1929, Apr. 2019.

[32] J.-C. Chou, Y.-X. Wu, P.-Y. Kuo, C.-H. Lai, Y.-H. Nien, S.-H. Lin, S.-J. Yan, and C.-Y. Wu, "Determination of L-ascorbic acid using MBs-AOX/GO/IGZO/Al by wireless sensing system and microfluidic framework," *IEEE Access*, vol. 7, pp. 45872–45880, Mar. 2019.

[33] J.-C. Chou, S.-J. Yan, Y.-H. Liao, C.-H. Lai, J.-S. Chen, H.-Y. Chen, T.-W. Tseng, and T.-Y. Wu, "Characterization of flexible arrayed pH sensor based on nickel oxide films," *IEEE Sensors J.*, vol. 18, no. 2, pp. 605–612, Jan. 2018.
[34] J.-C. Chou, J.-T. Chen, Y.-H. Liao, C.-H. Lai, R.-T. Chen, Y.-L. Tsai, C.-Y. Lin, J.-S. Chen, M.-S. Huang, and H.-T. Chou, "Wireless sensing system for flexible arrayed potentiometric sensor based on XBee module," *IEEE Sensors J.*, vol. 16, no. 14, pp. 5588–5595, Jul. 2016.
[35] S.-C. Tseng, T.-Y. Wu, J.-C. Chou, Y.-H. Liao, C.-H. Lai, J.-S. Chen, and M.-S. Huang, "Research of non-ideal effect and dynamic measurement of the flexible-arrayed chlorine ion sensor," *IEEE Sensors J.*, vol. 16, no. 12, pp. 4683–4690, Jun. 2016.
[36] S. E. Oraby and A. M. Alaskari, "Atomic force microscopy (AFM) topographical surface characterization of multilayer-coated and uncoated carbide inserts," *Int. J. Mech., Aerosp., Ind., Mech. Manuf. Eng.*, vol. 4, pp. 976–988, Mar. 2010.
[37] A. Sassolas, A. Hayat, and J.-L. Marty, "Immobilization of enzymes on magnetic beads through affinity interactions," in *Immobilization of Enzymes and Cells*, 3rd ed. J. Guisan, Ed. Totowa, NJ, USA: Humana Press, 2013, pp. 139–148.
[38] D. Yang, X. Wang, Q. Ai, J. Shi, and Z. Jiang, "Performance comparison of immobilized enzyme on the titanate nanotube surfaces modified by poly(dopamine) and poly(norepinephrine)," *RSC Adv.*, vol. 5, no. 53, pp. 42461–42467, Mar. 2015.
[39] H. Wang and S. Mu, "Bioelectrochemical response of the polyaniline ascorbate oxidase electrode," *J. Electroan. Chem.*, vol. 436, nos. 1–2, pp. 43–48, Oct. 1997.
[40] A. Fulati, S. M. U. Ali, M. H. Asif, N. H. Alvi, M. Willander, C. Brännmark, P. Strålfors, S. I. Börjesson, F. Elinder, and B. Danielsson, "An intracellular glucose biosensor based on nanoflake ZnO," *Sens. Actuators B, Chem.*, vol. 150, pp. 673–680, Oct. 2010.
[41] H. Nakazawa, R. Otake, M. Futagawa, F. Dasai, M. Ishida, and K. Sawada, "High-sensitivity charge-transfer-type pH sensor with quasi-signal removal structure," *IEEE Trans. Electron Devices*, vol. 61, no. 1, pp. 136–140, Jan. 2014.
[42] C. W. Liao, J. C. Chou, T. P. Sun, S. K. Hsiung, and J. H. Hsieh, "Preliminary investigations on a new disposable potentiometric biosensor for uric acid," *IEEE Trans. Biomed. Eng.*, vol. 53, no. 7, pp. 1401–1408, Jul. 2006.
[43] L. V. Rajaković, D. D. Marković, V. N. Rajaković-Ognjanović, and D. Z. Antanasijević, "Review: The approaches for estimation of limit of detection for ICP-MS trace analysis of arsenic," *Talanta*, vol. 102, pp. 79–87, Dec. 2012.
[44] L. Zhang, G. Wang, D. Wu, C. Xiong, L. Zheng, Y. Ding, H. Lu, G. Zhang, and L. Qiu, "Highly selective and sensitive sensor based on an organic electrochemical transistor for the detection of ascorbic acid," *Biosens. Bioelectron.*, vol. 100, pp. 235–241, Feb. 2018.
[45] K. Wang, J.-J. Xu, K.-S. Tang, and H.-Y. Chen, "Solid-contact potentiometric sensor for ascorbic acid based on cobalt phthalocyanine nanoparticles as ionophore," *Talanta*, vol. 67, pp. 798–805, Oct. 2005.
[46] J. C. B. Fernandes, L. T. Kubota, and G. D. O. Neto, "Potentiometric biosensor for l-ascorbic acid based on ascorbate oxidase of natural source immobilized on ethylene-vinylacetate membrane," *Anal. Chim. Acta*, vol. 385, pp. 3–12, Apr. 1999.
[47] M. Maccarrone and G. D'Andrea, M. L. Salucci, L. Avigliano, and A. Finazzi-Agrò, "Temperature, pH and UV irradiation effects on ascorbate oxidase," *Phytochemistry*, vol. 32, pp. 795–798, Mar. 1993.
[48] D. K. Kannoujia, S. Kumar, and P. Nahar, "Covalent immobilization of ascorbate oxidase onto polycarbonate strip for L-ascorbic acid detection," *J. Biosci. Bioeng.*, vol. 114, pp. 402–404, Jun. 2012.
[49] F.-G. Banica, *Chemical Sensors and Biosensors*, vol. 1, 1st ed. Hoboken, NJ, USA: Wiley, Jan. 2002, ch. 4, sec. 4.3, p. 111.
[50] D. R. Thévenot, K. Toth, R. A. Durst, and G. S. Wilson, "Electrochemical biosensors: Recommended definitions and classification," *Biosensors Bioelectron.*, vol. 16, pp. 121–131, Jan. 2001.
[51] D. Tonelli, B. Ballarin, L. Guadagnini, A. Mignani, and E. Scavetta, "A novel potentiometric sensor for l-ascorbic acid based on molecularly imprinted polypyrrole," *Electrochim. Acta*, vol. 56, pp. 7149–7154, Aug. 2011.
[52] N. M. Kocherginsky and Z. Wang, "Polyaniline membrane based potentiometric sensor for ascorbic acid, other redox active species and chloride," *J. Electroanal. Chem.*, vol. 611, pp. 162–168, Dec. 2007.
[53] P. G. Veltsistas, M. I. Prodromidis, and C. E. Efstathiou, "All-solid-state potentiometric sensors for ascorbic acid by using a screen-printed compatible solid contact," *Anal. Chim. Acta*, vol. 502, pp. 15–22, Jan. 2004.
[54] Z. H. Ibupoto, S. M. U. Ali, K. Khun, and M. Willander, "L-ascorbic acid biosensor based on immobilized enzyme on ZnO nanorods," *J. Biosens Bioelectron*, vol. 2, p. 110, Nov. 2011.

JUNG-CHUAN CHOU (SM'18) was born in Tainan, Taiwan, in July 1954. He received the B.S. degree in physics from Kaohisung Normal College, Kaohsiung, Taiwan, in 1976, the M.S. degree in applied physics from Chung Yuan Christian University, Chung-Li, Taiwan, in 1979, and the Ph.D. degree in electronics from National Chiao Tung University, Hsinchu, Taiwan, in 1988. From 1979 to 1991, he was a Lecturer, an Associate Professor, and the Director of the Department of Electronic Engineering, Graduate School of Electronic Engineering, Chung Yuan Christian University. Since 1991, he has been an Associate Professor with the Department of Electronic Engineering, National Yunlin University of Science and Technology, Yunlin, Taiwan, where he has been a Professor, since 2010. From 1997 to 2002, he was the Dean of the Office of Technology Cooperation, National Yunlin University of Science and Technology. From 2002 to 2009, he was the Chief Secretary with the National Yunlin University of Science and Technology. From 2009 to 2010, he was the Director of the Library, National Yunlin University of Science and Technology. From 2010 to 2011, he was the Director of the Office of Research and Development, National Yunlin University of Science and Technology. From 2011 to 2017, he was a Distinguished Professor with the Department of Electronic Engineering, National Yunlin University of Science and Technology. From 2013 to 2018, he was the Director of the Administration, Testing Center for Technological and Vocational Education. Since 2018, he has been the Deputy Director of the Headquarters, Testing Center for Technological and Vocational Education. Since 2018, he has been the Lifetime Chair Professor with the Department of Electronic Engineering, National Yunlin University of Science and Technology. His research interests include the areas of sensor material and device, biosensor and systems, microelectronic engineering, optoelectronic engineering, solar cell, and solid state electronics.

SI-HONG LIN was born in Taichung, Taiwan, in August 1995. He has received the B.S. degree from the Department of Electronic Engineering, National Yunlin University of Science and Technology, Yunlin, Taiwan, in 2017, where he is currently pursuing the M.S. degree with the Graduate School of Electronic Engineering. His current research interest includes biosensor applications.

PO-YU KUO (M'13) was born in Taichung, Taiwan, in 1980. He received the M.S. and Ph.D. degrees in electrical engineering from The University of Texas at Dallas, in 2006 and 2011, respectively. In 2013, he joined the Department of Electronic Engineering, National Yunlin University of Science and Technology, Yunlin, Taiwan, where he is currently an Assistant Professor. His research interests include the analog circuits, power management circuits, and analog circuit model analysis.

CHIH-HSIEN LAI (M'17) was born in Taichung, Taiwan, in 1968. He received the B.S. and M.S. degrees in electrical engineering, and the Ph.D. degree in photonics and optoelectronics from National Taiwan University, Taipei, Taiwan, in 1990, 1992, and 2010, respectively. He had worked in the telecommunications industry for a number of years, while working extensively with the Department of Electronic Engineering, Hwa Hsia Institute of Technology, Taipei, as an Assistant Professor, from 2004 to 2012. In 2012, he joined the Department of Electronic Engineering, National Yunlin University of Science and Technology, Yunlin, Taiwan, where he is currently a Professor. He has been serving as the Chairman of the Department of Electronic Engineering, since 2017. His current research interests include the optical and terahertz guided-wave structures, nanophotonic devices, and optoelectronic devices.

YU-HSUN NIEN (M'19) received the Ph.D. degree from the Department of Material Sciences and Engineering, Drexel University, Philadelphia, PA, USA, in 2000. He is currently a Professor and the Director of the Center for Industrial Pollution Prevention Research, National Yunlin University of Science and Technology, Yunlin, Taiwan. His research interests include materials engineering and sustainable energy development.

TSU-YANG LAI was born in Taoyuan, Taiwan, in January 1996. He received the B.S. degree from the Department of Communication Engineering, I-Shou University, Kaohsiung, Taiwan, in 2018. He is currently pursuing the M.S. degree with the Graduate School of Electronic Engineering, National Yunlin University of Science and Technology, Yunlin, Taiwan. His research interests include biosensor applications.

TZU-YU SU was born in Kaohsiung, Taiwan, in May 1996. She received the B.S. degree from the Department of Chemical Engineering, I-Shou University, Kaohsiung, Taiwan, in 2018. She is currently pursuing the M.S. degree with the Graduate School of Chemical and Materials Engineering, National Yunlin University of Science and Technology. Her current research interests include biosensor applications.